Proceedings of ASME Turbo Expo 2011
GT2011
June 6-10, 2011, Vancouver, British Columbia, Canada

GT2011-46461

APPLICATION OF AN EFFICIENT PRESSURE-TEMPERATURE COUPLED SOLVER TO INDUSTRIAL HYDRODYNAMIC BEARINGS IN CONJUNCTION WITH MULTI-OBJECTIVE EVOLUTIONARY OPTIMIZATION

V. Indriolo*, G. Melina, G. Ottino and G. Romanelli
Industry Division
CFD Engineering S.r.l.
P.za della Vittoria 7, 16121
Genova, Italy
indriolo@cfd-engineering.it

S. Minniti and F. Rindone
Turbomachinery Division
Ansaldo Energia S.p.A.
via N. Lorenzi 8, 16152
Genova, Italy
silvia.minniti@aen.ansaldo.it

ABSTRACT

Hydrodynamic bearings have a key role in the functioning of heavy duty gas turbines: they join a great vibration absorption with an efficient power dissipation by means of a film oil inserted between the turbo machine axes and the bearing case.

A classical approach for studying the functioning and the performance of this kind of bearings is to solve the so called Reynolds' equation, which is obtained from the Navier-Stokes equations under simplifying assumptions. As a result the pressure field is derived, the fluid film being considered isothermal: dissipation effects have to be estimated a posteriori in a post-processing procedure.

On the other hand a fluid environment having to be taken into account, a direct approach is carried out by the time consuming CFD analysis. After defining an appropriate mesh and choosing the appropriate solver, an almost exact solution of the entire flow field is obtained, that is pressure, velocity and temperature distributions. The main drawback is that the required time is several order greater than that required for the solution of the Reynolds' equation.

In the present work an alternative strategy is proposed, which consists of an iterative procedure: at each step the Reynolds' equation is solved in order to obtain the pressure field; a 1D energy balance is then applied along the length of the bearing for computing the temperature field. In this way the close relationship between pressure and temperature is modelled, the former depending on the oil viscosity locally changing with temperature, and the latter depending on the local oil mass flow and on dissipated power strictly correlated to the pressure distribution. The upgrading of both the entities ends when the convergence is reached.

Comparisons with literature test cases reveal the efficiency of the proposed technique: treating the interaction between pressure and temperature gives a solution which is very close to industrial configurations investigated, and at the same time the computational load is as light as that needed for the solution of the only Reynolds' equation. The performance of the above coupled solver can be greatly emphasised applying it to the bearing design. An integration with a multi-objective genetic optimization process is proposed, taking as objects to be optimized both geometrical and environmental variables. Application examples are shown about an industrial Ansaldo Energia lemon bore hydrodynamic bearing: given a currently applied configuration, possible improvements are suggested. Results are presented.

INTRODUCTION

Evaluation of static and dynamic performances of hydrodynamic bearings is mainly based on analytical or numerical approaches. The former use a closed-form solution of Reynolds' equation for circular bearing while the latter face the problem by means of distinct numerical techniques.

*Address all correspondence to this author.

If hypotheses of short or infinitely long bearings are verified, cases presented in [1] and [2] give simplified models applicable to industrial configurations. If not, hybrid closed solutions are also available in literature: [3] includes the effect of end leakage in short bearing by means of a correlation between experimental and numerical data; [4] proposes an harmonic pressure average technique applied to both long and short solutions to obtain valid results for any width.

Analytical simplifications could not be able to describe the reality with good agreement. An alternative is represented by Raimondi and Boyd chart method [5]: they numerically obtained graphics which enable the prediction of the bearing performances in conjunction with the oil temperature- viscosity relation. Developed in the fifties this approach is very time-efficient in front of its not so great accuracy. During the last decades further increase in accuracy has been obtained by means of different numerical solution techniques mainly based on FEM and CFD analysis. Examples of the former are, among the others, [6–9]: in addition to solving the three dimensional momentum, energy and continuity equations, finite element method is often applied to the analysis of fluid-solid interaction, thermo- elastic behaviour being considered in both the shaft and bush.

Furthermore if local fluid phenomena such as inertia, vorticity and turbulence have to be investigated, more in general great precision being needed, the CFD approach is essential. Problems raise related to thin geometries to be meshed, high pressure gradients and long computational time, but results are obtained in good agreement with reality [10–12]. A compromise between accuracy and time saving is to execute numerical campaigns [11] in order to create charts available in future design phases without needing to perform a specific CFD analysis each time.

An important aspect to be taken into account in predicting bearing performances is the thermal one. Since the first half of the past century it is well known the influence of temperature on viscosity and density of the lubricating oil, the latter being negligible with respect to the former [13]. Another effect, also due to thermal fluxes between the lubricant and the shaft-case structure, is thermo-elastic deformation, deeply investigated, among the others, in [14, 15].

The aim of this work is to present a tool useful in the initial design process of journal bearings based on a fast procedure assuring an acceptable accuracy in comparison with experimental data. An approach is described which enables a time saving computing of hydrodynamic bearing performances. Assumptions are made which reduce the study of the flow field characterising the lubricating film to the solution of the classical 2D Reynolds' equation [16–18]. The formulation does not take into account fluid inertia and shaft/bush elastic deformation. As showed in [19] the fluid inertia does not significantly affect the pressure field. [20] suggests that influence of thermal and elastic deformations are negligible in a first approximation when computing performances of journal bearings operating under full hydrodynamic regime. On the other side viscosity variations are modelled by means of their dependence on the temperature field. In literature pressure-temperature coupling is treated in several ways, as indicated in [21] and references therein. In the present work a simple algebraic relation is used which relates the dissipated power at the oil-shaft/case interfaces to the temperature variation with respect to the supply condition. Adiabatic assumptions are made, the thermal increase being completely carried out of the bearing only by the fluid film [22]. The temperature variations are evaluated at each axial section which the geometry is discretised into: an average value is computed which enables an increased accuracy in term of global load in spite of less accurate local results. More precise numerical predictions could be obtained considering temperature variations along and across the fluid film thickness [23]; however a great increase in the computational load would be unavoidable, leading this modelling out of the purpose of this work.

When no complex geometries have to be dealt with, Finite Difference Method (FDM) is surely one of the best to be used thanks to accuracy and efficiency and to short computational time. In the present paper an iterative procedure is built up and implemented, which requires the FD solution of the Reynolds' equation followed by the computation of the temperature variations; a new viscosity value is then computed and put into the Reynolds' equation, which has to be solved again. And so on until the convergence is reached. Results in good agreement with experimental data are shown. In particular, it can be seen how segregated approach, separating the mutual influence of pressure and temperature fields, overestimates minimum oil film thickness leading to too conservative results.

In the last section an application of the implemented tool is shown in conjunction with an optimization technique. The genetic approach is selected due to its capability to directly capture the absolute minimum zone even if high non-linearities are present; a better technique would consist in an hybrid strategy, combining an evolutionary algorithm to a gradient-based one, the former finding the minimum zone, the latter increasing the local accuracy [24, 25]. According to the aim described above, the hybrid strategy could require too much computational time, and so it is not adopted preferring the genetic algorithm which is simpler to be implemented, faster and completely independent from the starting set of values. Results are shown which demonstrate the ability of the tool to reproduce real industrial configurations.

THERMO-FLUID DYNAMICS MODELLING

According to targets previously indicated, choosing the appropriate combination of mathematical model and numerical solution strategy is fundamental in order to provide the best compromise between accuracy, simplicity and computational efficiency.

In the design phase it is often necessary to run hundreds or

even thousands of simulations to gain a complete insight over the static and dynamic behaviour of the component under analysis. With this idea in mind we choose not to resort to Computational Fluid Dynamics (CFD) solvers of the (compressible) Reynolds' Averaged Navier Stokes (RANS) equations and the turbulence model equations. This is because of a number of reasons, e.g.: a) the complication of building a numerical mesh to discretize the small fluid layer between the rotating journal and the housing, b) the significant CPU time required by a CFD simulation to complete and c) the excessive information content delivered by CFD tools, almost useless to carry out a global static and dynamic characterization of the journal bearing.

In order to overcome those issues we choose the simplified mathematical model of the Reynolds' equation and we implement from scratch a new dedicated computational kernel with the target of achieving a high level of: a) simplicity, b) computational efficiency, c) accuracy in terms of global quantities (e.g. forces, equilibrium position, hydrodynamic stiffness and damping matrices), d) flexibility (e.g. broad gamma of bearing geometries) and e) customizability (e.g. possibility to add new fluid types).

In Fig. (1) a schematic drawing of a circular journal bearing is presented, but it can be used as a reference for any bearing geometry here considered. First of all it is useful to introduce three major classes of parameters that will be used throughout the paper: a) geometric parameters such as the journal radius R, the bearing length L and the housing clearance C, b) parameters linked with the working conditions, such as the journal angular velocity Ω, the reaction load acting on the bearing W and pressure P_{ref} and temperature T_{ref} of the lubricant supply system and finally c) parameters specifying the type of oil used, such as density ρ, dynamic viscosity μ and heat coefficient C_v. As a function of the equilibrium position or eccentricity, known in terms of magnitude e and attitude angle ϕ, it is then possible to compute the film layer thickness $H(e,\phi)$. It is also important to remark that the origin of the coordinate system $x-y-z$ is located at the center of the bearing (with the x axis aligned to gravity vector).

As clearly derived in [26] the Reynolds' equation governing the pressure distribution $P = P(\theta,z)$ in the newtonian lubricant film of a journal bearing can be written as the following Partial Differential Equation (PDE):

$$\frac{1}{R}\frac{\partial}{\partial\theta}\left(\frac{H^3}{12\mu}\frac{\partial P}{\partial\theta}\right)+\frac{\partial}{\partial z}\left(\frac{H^3}{12\mu}\frac{\partial P}{\partial z}\right)=\frac{\partial H}{\partial t}+\frac{\Omega}{2}\frac{\partial H}{\partial\theta}. \qquad (1)$$

To complete the statement of the problem the boundary conditions are specified as follows:

- periodicity with respect to θ, that is $P(\theta+2\pi,z)=P(\theta,z)$,
- symmetry at $z=0$, that is $\partial P/\partial z(\theta,0)=0$ and
- fixed uniform value at $z=\pm L/2$, that is $P(\theta,\pm L/2)=P_{\text{ref}}$.

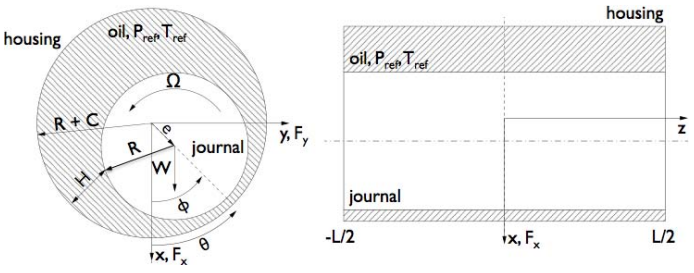

FIGURE 1. SCHEMATIC DRAWING OF A JOURNAL BEARING.

Once Eqn. (1) is solved and the pressure distribution P is known, it is straightforward to compute the global hydrodynamic forces exchanged between the lubricant film and the journal, projected along the radial and tangential unit vectors respectively, as follows:

$$F_r = 2\int_0^{L/2}\int_0^{2\pi} P(\theta,z)\cos\theta\, R\mathrm{d}\theta\mathrm{d}z \qquad (2)$$

$$F_t = 2\int_0^{L/2}\int_0^{2\pi} P(\theta,z)\sin\theta\, R\mathrm{d}\theta\mathrm{d}z \qquad (3)$$

where the integral is computed only on half bearing and the result is then multiplied by a factor two exploiting the symmetry of the solution across the longitudinal axis. Finally the forces can be written in the global reference frame applying the following transformation:

$$F_x = F_r\cos\phi - F_t\sin\phi \qquad (4)$$

$$F_y = F_r\sin\phi + F_t\cos\phi \qquad (5)$$

In order to model cavitation negative values of the pressure P are simply set equal to zero. Although this strategy causes discontinuities in the flow of the lubricant film (with minor side effects on the computation of derived quantities, such as mass flow or viscous stresses), it is easy to implement as compared to the more realistic approach in which continuity is imposed at the boundary of the (unknown) cavitation area [27]. In fact in this latter case the problem would become non-linear.

It is also useful to remark that Eqn. (1) is linear for an isothermal lubricant and a rigid journal. In the case of a non-isothermal lubricant the problem becomes non-linear since the pressure distribution P depends on the dynamic viscosity μ of the lubricant film, which in turn depends on the temperature T of the lubricant film, which in turn depends on the power $\mathscr{D}$ dissipated by the tangential stresses, that is, in compact notation $P(\mu(T(\mathscr{D}(P))))$. Similarly in the case of bearing wall deformation P depends on the lubricant film thickness H, which in turn depends on the deformation $\mathscr{E}$ of the journal due to the hydrodinamic loads, that is, in compact notation $P(H(\mathscr{E}(P)))$.

According to the assumptions described above and considering the high in-plane stiffness of journal sections of heavy-duty turbomachinery applications, the modelling of elastic deformations is not performed. On the other hand the treatment of the interaction between Reynolds' and heat equations (governing respectively pressure and temperature distributions) is expected to provide a better insight of the physics of the phenomenon, since the very strong dependency of viscosity on temperature.

Roughly speaking, the goal is to switch from an isothermal lubricating film - characterised by an *a priori* temperature value - to a model based on the mutual interaction between temperature and flow-field. To this end, together with Eqn. (1) we iteratively solve a very simplified version of the heat equation for the longitudinal temperature distribution: the constitutive assumption is that all the power $\mathscr{D}$ dissipated by viscous friction at lubricant-journal interface is carried out of the bearing by convection by means of the oil mass flow rate. The resulting equation is:

$$\rho C_v Q \Delta T = \mathscr{D} \tag{6}$$

where Q is the section-averaged axial mass flow computed as a function of the pressure distribution as in [26], and ΔT represents the temperature differential with respect to the supply conditions. This equation is applied independently at each i-th longitudinal section of discretisation, the computation of $\mathscr{D}_i$ being performed as follows:

$$\mathscr{D}_i = \int_{z_i}^{z_{i+1}} \int_0^{2\pi} \tau R \Omega R d\theta dz \quad \text{with} \quad \tau = \frac{\mu \Omega R}{H} + \frac{H}{2R}\frac{\partial P}{\partial \theta}. \tag{7}$$

According to this strategy each of the N_i sections is characterised by a constant temperature value. In this way there is an unavoidable loss of accuracy on temperature distribution along and across the single section. However, according to the aim of the work this is acceptable thanks to the improvement obtained in global evaluations, as can be seen in following paragraphs. This iterative P-T coupling procedure is summarized in Fig. (2).

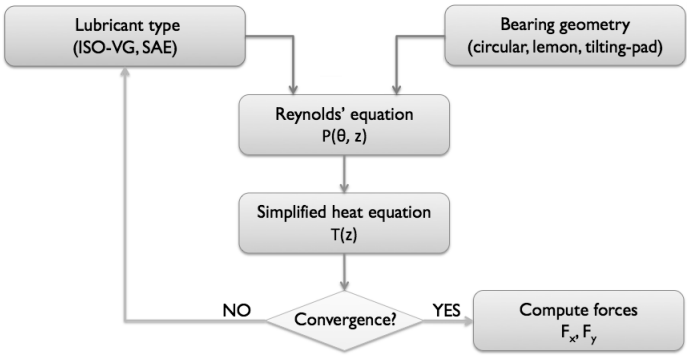

FIGURE 2. NON-LINEAR P-T COUPLING PROCEDURE.

COMPUTATIONAL KERNEL

In general it is not possible to find an analytical solution to Eqn. (1). However under specific assumptions it is possible to further simplify the mathematical model of the Reynolds' equation in such a way that an analytical approach is actually feasible. For example for circular *short* bearings with a length-diameter ratio $L/D \leq 1/2$ the pressure gradient in the circumferential direction can be neglected in comparison to the pressure gradient in the axial direction, so that the first term on the left-hand side of Eqn. (1) can be discarded. Similarly for perfectly sealed circular *long* bearings with a length-diameter ratio $L/D > 2$ the pressure can be assumed constant in the axial direction, so that the second term on the left-hand side of Eqn. (1) can be discarded. In both cases it is relatively easy to compute the exact solution. However predictions would be obtained under too restrictive assumptions to deliver satisfactory results for real-world problems too. At the same time they could be useful for validating a numerical solution algorithm.

To solve the Reynolds' equation (optionally coupled with the simplified heat equation) for industrial journal bearings without making simplifying geometrical assumptions, we implemented in C^{++} a Finite Difference (FD) solver. The toolbox is made by the following ingredients:

preProcessing: collection of functions devoted to the setting of the case to be run. In particular it includes:

a) generation of a 2D cartesian grid on the domain $(\theta, z) = (0, L/2) \times (0, 2\pi)$ as shown in Fig. (3), making symmetry assumptions in order to discretise only a half of the bearing. Index i is associated to θ coordinate in such a way that $\theta_i = i\Delta\theta$ and $\theta_{N_i} = 2\pi$. Analogously index j is associated to z coordinate so that $z_j = j\Delta z$ and $z_{N_j} = L/2$.

b) utilities able to compute the lubricant film thickness $H(\theta)$ as function of the angular coordinate θ, given the eccentricity magnitude e, the attitude angle ϕ and the type of bearing. At the same time some utilities are dedicated to check input data by computing the area of admissible displacements of the journal.

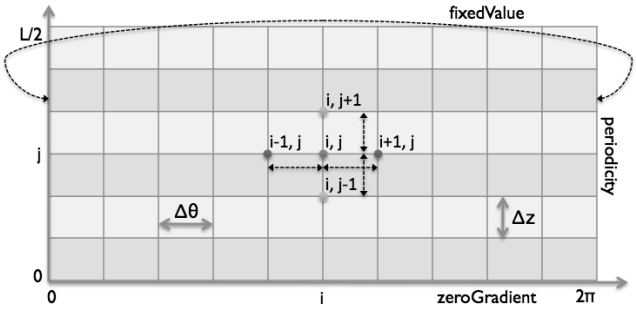

FIGURE 3. NUMERICAL GRID AND FD DISCRETIZATION.

solveReynoldsEquation: kernel of the toolbox dedicated to the Finite Differences (FD) 5-point stencil discretization of Eqn. (1), readily:

$$\frac{H^3_{i+1/2}P_{i+1,j} - (H^3_{i+1/2} + H^3_{i-1/2})P_{i,j} + H^3_{i-1/2}P_{i-1,j}}{12\mu R^2\Delta\theta} + H^3_i \frac{P_{i,j+1} - 2P_{i,j} + P_{i,j-1}}{12\mu\Delta z} = \frac{\Omega}{2}\frac{H_{i+1} - H_{i-1}}{2\Delta\theta} + \frac{\partial H}{\partial t} \quad (8)$$

To make easier the assembly of the left-hand side sparse matrix A and the right-hand side array b a small utility has been developed in order to handle the connectivity from the 2D numerical grid to the 1D solution array ordering and to impose the appropriate boundary conditions. The resulting linear system $Ax = b$ is solved by means of a dedicated opaque class wrapping the direct and iterative sparse linear solver libraries UMFPack and PETSc.

solveHeatEquation: function dedicated to the evaluation of all pressure-derived quantities, e.g. mass flows, tangential viscous stresses, etc., and finally to the solution of the simplified heat equation Eqn. (6).

solveLoads: function dedicated to the computation of the global forces exchanged between the journal and the lubricant film, projected onto both the radial and tangential unit vectors and the global frame of reference.

STATIC ANALYSIS

Given a set of geometric parameters, working conditions and lubricant type, the main target of the static analysis is the determination of equilibrium position of the journal in steady motion in such a way that the global forces balance the journal reactions, that is $F_x = -W$ while $F_y = 0$. The relative position of the journal axis with respect to the center of the housing is conventionally identified by means of eccentricity magnitude e and attitude angle ϕ. This eccentricity of the shaft provides the non-symmetry of H with respect to the x and y axes, which is responsible of the hydrodynamic loads generation.

Resulting from Eqn. (4-5), this problem is non-linear because of the non-linear dependency of forces F_x and F_y on the eccentricity magnitude e and attitude angle ϕ. Therefore in general it must be solved by means of a costly iterative procedure. However in case of circular bearings it is easy to show that the radial and tangential projections of the hydrodynamic loads depend exclusively on the eccentricity magnitude e and not on the attitude angle ϕ. This simplifies significantly the problem which can now be solved with e.g. a bisection procedure on e; on the other hand the attitude angle is computed in such a way that the equilibrium along the horizontal direction is satisfied, that is: $\phi = \text{atan}(-F_t/F_r)$.

For generic bearing geometries the problem is more complex and costly. We implemented an iterative adaptive search method in which the equilibrium position is determined on a very coarse grid of candidate values $(e_{\min}, e_{\max}) \times (\phi_{\min}, \phi_{\max})$. Minimum and maximum positions are initialized in such a way that contact or non-physical phenomena do not occur, and are progressively shrinked in the neighbourhoods of the resulting best candidate. This procedure eventually converges to the equilibrium position. Of course it is significantly more costly than the simple bisection procedure set-up for circular bearings.

Together with the determination of the equilibrium position of the journal, during the static analysis it could be required to build a map of the global forces F_x and F_y as function of the free parameters e and ϕ. In fact the availability of those static maps provides a better insight on the problem, focusing in particular on the sensitivity of the global forces to the position of the journal. Such an information is very important for example to prevent dangerous contact phenomena.

DYNAMIC ANALYSIS

Given a set of geometric parameters, working conditions and lubricant type, the main target of the dynamic analysis is the determination of the hydrodynamic damping C and stiffness K matrices. These 2×2 matrices are computed locally linearising F_x and F_y forces with respect to perturbations of the position Δx and Δy and of the velocity $\Delta\dot{x}$ and $\Delta\dot{y}$ around the equilibrium position previously defined; readily:

$$K_{i,j} = \frac{\partial F_i}{\partial x_j} \qquad \text{and} \qquad C_{i,j} = \frac{\partial F_i}{\partial \dot{x}_j}, \quad (9)$$

they are numerically evaluated by means of a Finite Difference (FD) strategy. Together with the mass matrix $M = \text{diag}(W/g)$ it is now possible to build the following Reduced Order Model (ROM) of the dynamics of the journal-bearing coupled system:

$$M\ddot{q} + C\dot{q} + Kq = F_{\text{ext}}, \quad (10)$$

where q is the array of the 2 degrees of freedom Δx and Δy, while F_{ext} is the array of the external perturbation forces acting on the journal. These data are sufficient to perform the following two types of complementary analyses:

stability analysis: the task is to understand if the journal-bearing coupled system will return to the stable configuration or diverge from it after applying a perturbation, as shown in Fig. (4). To this end it is sufficient to examine the eigenvalues of equation Eqn. (10) in homogeneous form and check if there exists at least one eigenvalue having a positive real part (unstable case) or not.

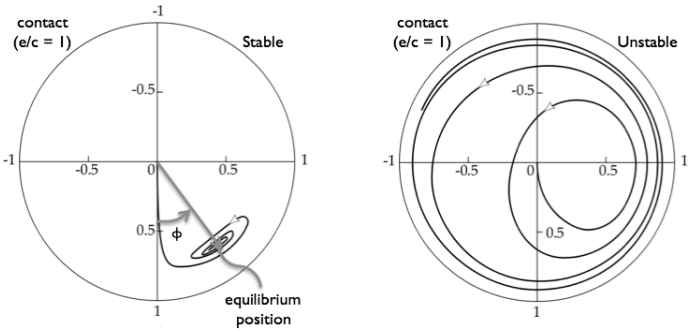

FIGURE 4. STABLE AND UNSTABLE TRAJECTORIES.

response analysis: the task is to simulate the dynamic behaviour of system Eqn. (10) when an external perturbation on the initial conditions or on the external forces is applied. In this way it is possible to check if during the start-up phase from the bearing centerline to the journal equilibrium position possible overshooting phenomena lead to contact.

Both these analyses are fundamental in the design phase, since they provide a lot of useful data for handling e.g. the start-up phase or off-design conditions.

OPTIMIZATION TECHNIQUES

The development (design, implementation and integration) of new cost-effective numerical methods for automatic shape optimization has been a very fruitful research field during the last two decades, because of the complexity and the importance of the problem under analysis.

Probably the most widespread strategy for solving such a problem consists in the so called *Gradient Methods* (GM). The idea can be summarized as follows: given a smooth and convex functional $J(x)$ where x is the set of the N_x design parameters or degrees of freedom of the problem, in order to find the optimal solution x such that the value of the functional J is minimized, it is convenient to follow the direction of the gradient ∇J in the parameter space. From a computational point of view this implies at least $2N_x$ evaluations of the functional J in order to build an approximation of the gradient ∇J by means of a first order accurate non-centered Finite Differences (FD) scheme.

An alternative to these methods is offered by *Genetic Algorithms* (GA). The idea can be summarized as follows: the optimal solution x such that the value of the functional J is minimum is determined exploiting the analogy between an optimization problem and the theory of evolution. During each single iteration of the optimization process the design parameters, also called *genes* in such a context, are suitably modified by means of the *selection*, *recombination*, *cross-over* and *mutation* operators in such a way that only the fittest elements of the initial random population do survive.

With respect to gradient methods, this latter optimization strategy does not require any specific hypothesis regarding the regularity of the functional J and it is effectively applied to problems with both real and integer degrees of freedom. Another great advantage is its independency from initial guess parameters: regardless of their values, the strategy is not influenced by local minima, giving directly the absolute optimal solution even if the system to be analised is completely unknown. On the other hand it is possibile to show that the number of functional evaluations needed by a genetic algorithm is usually greater than the corresponding number of functional evaluations needed by a gradient method. However this overhead is mitigated by the available actual computing power and by the possibility of distributing computational effort on parallel configurations. Moreover the GA strategy is definitely more suited to tackle *multi-objective* design problems, such as the design of the optimal geometry of a hydrodynamic bearing. In fact the word *optimal* in this case is in general a very complex mix of static and dynamic required performances and/or geometrical constraints. Therefore we choose to implement in C^{++} the genetic optimization tool GenOpt as described in [28].

However it is important to specify the reader about the aim of this work: the target is not to show the performance of a genetic algorithm with respect to the other available techniques, but rather to demonstrate that the above implemented approach for predicting journal bearing performances could be easily and effectively inserted into a generic optimization strategy, as it is demonstrated by results shown in next sections. This is a further aspect which demonstrate the capability of the implemented tool of supporting the design process.

A short description of the single phases of the optimization process is now presented. It is easy to see by the labelling names that they mimic the single stages of the biological evolution of a population of living organisms. The fundamental idea in GA consists in describing the space of design parameters by means of N_g *genes*: you denote the i-th gene of the n-th generation as X_i^n. A given set of genes completely identifies an individual of the population, also called *chromosome*: more in particular the j-th chromosome of the n-th generation can be written as follows:

$$\mathscr{X}_j^n = \left\{ X_1^n, X_2^n, \ldots, X_{N_g}^n \right\}. \tag{11}$$

To start the genetic optimization process it is necessary to define the initial generation G^0, which can be represented as the following combination of N_c chromosomes:

$$G^0 = \left\{ \mathscr{X}_1^0, \mathscr{X}_2^0, \ldots, \mathscr{X}_{N_g}^0 \right\}. \tag{12}$$

Without any specific information a random initialization compatible with the specified constraints is chosen.

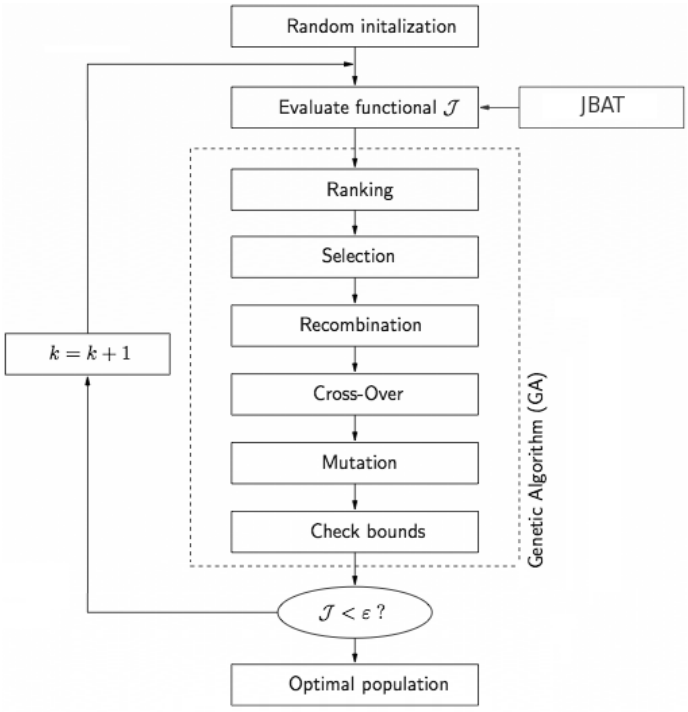

FIGURE 5. GENETIC OPTIMIZATION ALGORITHM.

With reference to Fig. (5), at each n-th iteration (which corresponds to a new generation) it is now necessary to execute the following operations:

Ranking: it orders the chromosomes of the current population in decreasing order starting from the most optimal to the least fit, depending on the value of the functional $J(\mathscr{X}_j^n)$.

Selection it chooses the fittest chromosomes of the current generation depending on the associated ranking index.

Passthrough it lets the first n_p fittest chromosomes pass unaltered (copied as is) to the next generation.

Cross-over it sets the value of n_{co} chromosomes as the arithmetic average of two randomly chosen chromosomes.

Perturbation Mutation it applies a random perturbation to the value of n_{pm} genes in the current generation without violating the prescribed contraints.

Mutation it randomly resets the value of n_m genes in the current generation.

All the steps must be repeated until a satisfactory level of convergence is reached. It is important to remark that if we choose a greater number of chromosomes N_c the optimization process will probably converge in a smaller number of iterations. However the computational cost per iteration will be greater because of the increased number of functional evaluations.

With respect to the algorithm described in [28,29] we implemented a novel strategy to handle adaptive constraint boundaries to drive the optimization algorithm towards convergence faster. This result is obtained as follows: as the numerical minimization procedure delivers a better and better solution the boundaries for the random number generator are progressively reduced in such a way that operations such as Mutation always cooperate to drive the solution towards the optimum and do not simply introduce the same level of *noise* in the initial generation and in a generation very close to the optimal one. Practically speaking, at each n-th iteration the maximum $\mathscr{H}_i$ and minimum $\mathscr{L}_i$ constraints relative to each i-th gene are adjusted as follows:

$$\mathscr{H}_i^{n+1} = \mathscr{O}_i^n - \frac{\delta}{2}(\mathscr{H}_i^n - \mathscr{L}_i^n) \tag{13}$$

$$\mathscr{L}_i^{n+1} = \mathscr{O}_i^n + \frac{\delta}{2}(\mathscr{H}_i^n - \mathscr{L}_i^n) \tag{14}$$

where $\mathscr{O}_i^n$ is the value of the i-th gene belonging to the best fitted chromosome into the current population, and δ is a suitable scalar coefficient defined by the user. In this way the successive iteration is performed on an admissible range which is closer to the final optimum result.

A set of possibile functionals to be used in conjunction with the toolbox named JBAT is now presented for the automatic shape design of journal bearings. A generic functional can be viewed as a weighted sum of performance indices (deviation from the target value) and constraints (Lagrange's multipliers) as follows:

$$J(x) = \sum_{i=0}^{P} W_i |y_i - y_i^{\text{target}}| + \sum_{j=0}^{C} \Lambda_j |z_j > z_j^{\text{target}}| \tag{15}$$

In the framework of journal bearing applications Eqn. (15) must be suitably specialized depending on the kind of computation which it is used in conjunction with; in particular in static computations forces could be token as reference because, in the direct procedure, they are the results of the P-T coupled iterative procedure based on specific geometrical inputs. On the other side in the dynamic cases attention could be more conveniently paid to the response of the system to external forces, that is, damping and stiffness properties, the former affecting the time needed to reach the equilibrium position, the latter the equilibrium position itself. For instance:

a) when dealing with a single-run performance prediction, it is straightforward for the user to specify the desired target forces F_x^{target} and F_y^{target}. Properly it is reasonable to use the target forces as weights, that is:

$$J(x) = \frac{|F_x - F_x^{\text{target}}|}{F_x^{\text{target}}} + \frac{|F_y - F_y^{\text{target}}|}{F_y^{\text{target}}}, \tag{16}$$

b) when a global static performance has to be satisfied, it is convenient to specify the desired target equilibrium position in terms of eccentricity e and attitude angle ϕ, or even more realistically the maximum acceptable eccentricity $e^{\max}$ (to prevent and monitor potentially dangerous near-contact phenomena) without loosing the ability of balancing the weight of the journal ($Fx = -W$ and $F_y = 0$), that is:

$$J(x) = \frac{|F_x - W|}{W} + \frac{|F_y|}{W} + |e < e^{\max}|, \qquad (17)$$

c) when a global dynamic performance has to be satisfied, the user can choose between two alternatives as above said, that is, optimizing on either the damping or the stiffness coefficients: if its aim is to modify the system time/overshooting response, he has to specify the desired target level of hydrodynamic damping coefficient C_{xy}, or even more realistically a desired target norm of the hydrodynamic damping matrix $\|C\|$ together with a static constraint on the maximum acceptable eccentricity $e^{\max}$, that is:

$$J(x) = \frac{|\|C\| - C^{\text{target}}|}{C^{\text{target}}} + |e < e^{\max}|. \qquad (18)$$

BENCHMARK TEST PROBLEMS

A validation of the analysis and optimization toolbox presented in the previous sections is now carried out by means of a series of comparisons with literature data and real industrial applications. First a test case verifying geometrical made assumptions is evaluated analytically and numerically both with an isoviscous and temperature-dependent fluid. Then a lemon bore bearing for heavy gas turbines applications is analyzed and results are discussed. Finally an example of the capabilities of the automatic shape optimization toolbox are presented. The lubricant types used are the SAE 40 and the ISO-VG 46 [30].

CIRCULAR BEARING

Static equilibrium is evaluated for the circular bearing shown in Fig. (1) with a ratio $L/D = 1/2$. The journal has a radius $R = 40$ mm, a weight 9000 N and a speed of rotation $\Omega = 60$ rps. The bearing is fed with an inlet pressure $P_{\text{ref}} = 1$ bar and temperature $T_{\text{ref}} = 65\ ^\circ$C.

Fig. (6) (on the left) represents the hydrodynamically generated pressure profiles at the mid-plane of the bearing for the three different models. First, it is possible to note that all solutions place the rupture zone at the same angular position. Particularly, the analytical approach indicates cavitation of oil by means of negative values while numerical schemes saturate those that are less than the oil film rupture. Differences are present in the sector where pressure is positive. With reference to maximum pressure, the T-fixed fluid assumption shifts the peak, while analytical and coupled solutions are closer both in terms of angular shift and magnitudes. A better visualization of axial and circumferential contour is also proposed in Fig. (6) (on the right) where it is possible to appreciate that absolute peak occurs at the bearing mid-plane.

Finally in Fig. (7-8) the results of the static and dynamic analyses are presented in order to highlight the major differences between the segregated and coupled algorithms. In the first one force isolines are plotted into the eccentricity geometrical space; the intersection of the isolines $F_x = -W$ and $F_y = 0$ gives the working equilibrium position of the shaft, the black point being related to the P-T coupling technique proposed and the red one to a fixed temperature computation. The second figure represents the time response of the linearized journal-bearing dynamic system starting from a central position. From both the figures it can be noted that the procedure with fixed temperature is less conservative with respect to the coupled one.

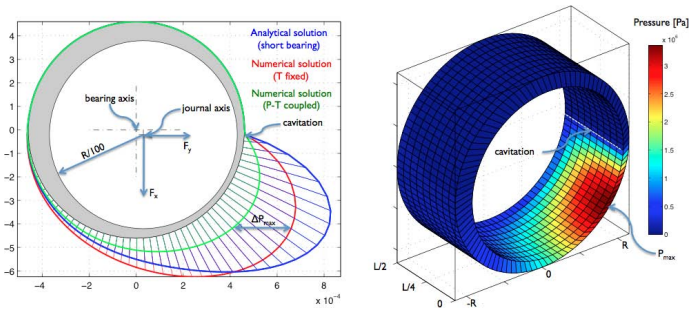

FIGURE 6. PRESSURE DISTRIBUTION INSIDE THE BEARING AS PREDICTED BY THE P-T COUPLED PROCEDURE.

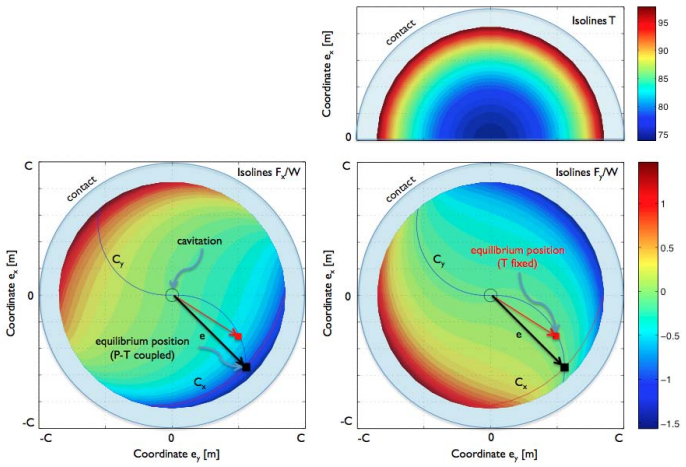

FIGURE 7. STATIC ANALYSIS MAPS: PEAK TEMPERATURE ISOCONTOURS (upper right), F_x/W ISOCONTOURS (lower left), F_y/W ISOCONTOURS (lower right)

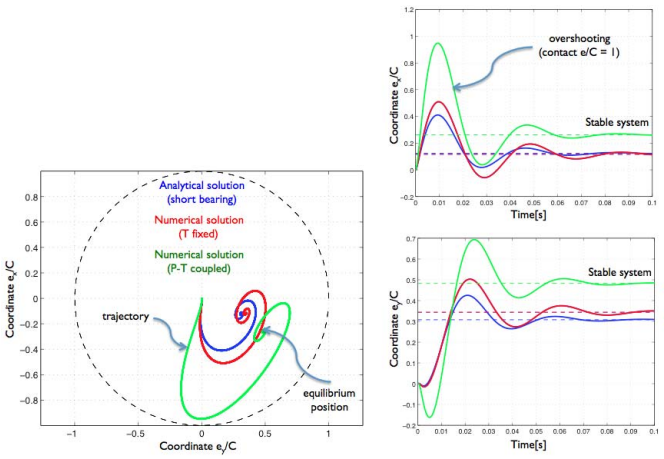

FIGURE 8. DYNAMIC RESPONSE, START-UP SIMULATION.

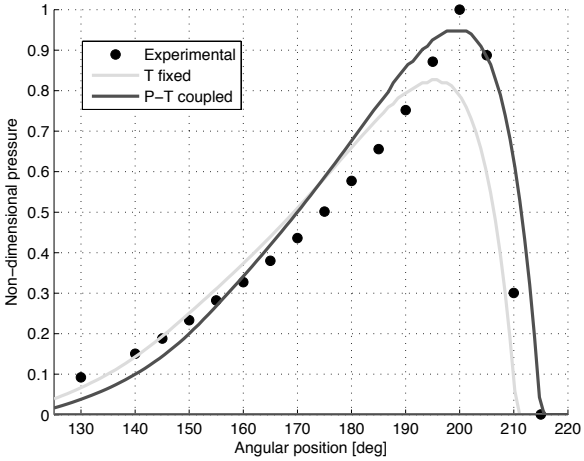

FIGURE 9. COMPUTED PRESSURE DISTRIBUTIONS AND COMPARISON WITH EXPERIMENTAL DATA.

LEMON BEARING

The compressor side journal bearing belonging to the gas turbine is composed by two halves with a maximum vertical clearance of $C = 0.8$ mm. An effective bearing length of $L = 300$ mm and a rotor radius of $R = 400$ mm are measured fixing the ratio $L/D = 0.75$. The load applied is $W = 360688$ N and the journal rotates at the angular velocity $\Omega = 3000$ rpm. Supply conditions are $T_{\text{ref}} = 28.7\ ^{\circ}\text{C}$ and $P_{\text{ref}} = 1.48$ bar. The measurements are performed in an overspeed chamber characterised by a pressure of almost $P_0 = 6.03$ mbar by means of relative pressure sensors placed in the lower part of the shaft at the mid-plane section into the white metal of the case.

Values showed in Fig. (9) are non-dimensionalized with respect to the maximum pressure acquired. As shown a better agreement between test and numerical model is assured by the P-T coupled solver both in terms of magnitudes and angular positions. In fact higher pressures and a more precise disposition of oil rupture are assured, while a shift that forwards both peak and oil cavitation is noticeable in the analytical short bearing model. Finally it is also important to remark that the peak temperature computed numerically at the mid-plane bearing section $T_{\text{peak}} = 50.3\ ^{\circ}\text{C}$ is close to the peak temperature evaluated during the experimental campaigns $T^{\text{exp}}_{\text{peak}} = 51.6\ ^{\circ}\text{C}$ with a relative error equal to $\varepsilon = 2.5\%$

SHAPE OPTIMIZATION

With reference to the circular bearing geometry presented in Fig. (1), we now present a simple but representative application of automatic shape optimization. Starting from the results of the static analysis previously run it is assumed that the bearing radius R and the journal angular velocity Ω are not known. Therefore R and Ω are chosen as degrees of freedom, and the genetic optimizer is set in order to find the optimal values of those parameters satisfying a particular single-run performance as in Eqn. (16), that is, to obtain $F_x = -W$ and $F_y = 0$. Actually it is already known the answer to this question, that is, $R = 0.04$ m and $\Omega = 376.99$ Hz, so this shape optimization example can be used as an accuracy and efficiency benchmark.

In Fig. (10) the convergence history of the inverse of the functional $F = 1/J$ is presented. It is possible to appreciate that the application does not converge to the optimal solution in a monotone way. More in particular a big step towards the optimal solution is done during the first 200 iterations, while successively the solution is progressively refined with minor and minor corrections. It is also interesting to note that the envelope of the maxima of F is characterized by sudden jumps after a number of iterations during which the solver seems to be stalled but it is actually exploring new possibile solutions.

In Fig. (10) the convergence history of the degrees of freedom is shown, together with a zoom on the last 50 iterations. It is possible to see how the adpative boundary feature drives the optimizer towards a faster convergence and that the final solution is actually the correct one equal to $R = 0.04$ m and $\Omega = 376.99$ Hz.

CONCLUSIONS

In this paper the design and implementation in C^{++} of a toolbox is presented, which is able to analyse in an efficient way the static and dynamic characteristics and automatically optimize the shape of real-world journal bearings. The main features of the toolbox were benchmarked on a series of simple but representative test problems.

Existing deviations between the coupled P-T algorithm and data acquired can be related to current modeling criteria implemented. Local phenomena like biphase fluid in rupture region, rotor axis misalignment and thermal deformations are not yet modelled at this stage of development and could provide better results closer to the experimental ones.

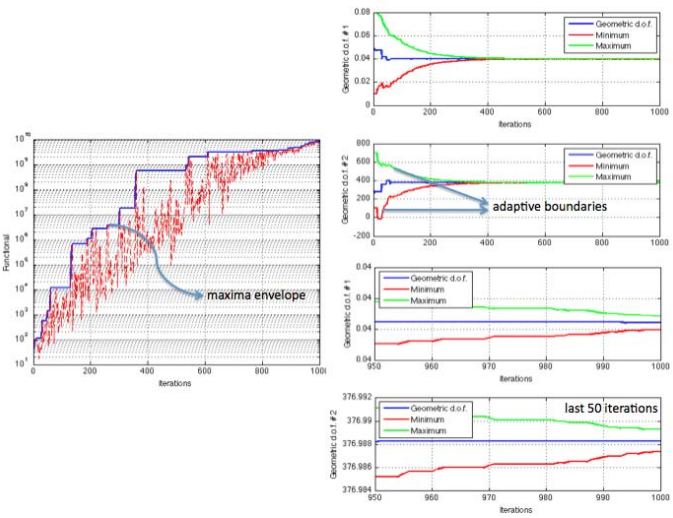

FIGURE 10. CONVERGENCE HISTORY OF THE FUNCTIONAL $F = 1/J$ AND THE DEGREES OF FREEDOM.

REFERENCES

[1] Sommerfeld, A., 1904. "Zur hydrodynamischen theorie der schmiermittelreibung". *Z. Math. Phys.,* ***50***, pp. 97–155.

[2] Ocvirk, F., and NACA, 1952. *Short-Bearing Approximation for Full Journal Bearings*. NACA Technical Note 2808.

[3] Dubois, G., Ocvirk, F., and NACA, 1953. *Analytical Derivation and Experimental Evaluation of Short-Bearing Approximation for Full Journal Bearings*. National Advisory Committee for Aeronautics.

[4] Reason, B., and Narang, I., 1982. "Rapid design and performance evaluation of steady-state journal bearingsa technique amenable to programmable hand calculators". *Taylor & Francis Trib. Trans.,* ***25***(4), pp. 429–444.

[5] Raimondi, A., and Boyd, J., 1958. "A solution for the finite journal bearing and its application to analysis and design: III". *Taylor & Francis Trib. Trans.,* ***1***(1), pp. 194–209.

[6] Indulekha, T., Joy, M., and Nair, K., 1994. "Fluid flow and thermal analysis of a circular journal bearing". *Springer Heat Mass Transf.,* ***29***(6), pp. 367–371.

[7] Gethin, D., 1985. "An investigation into plain journal bearing behaviour including thermo-elastic deformation of the bush". *Proc. of the Institution of Mechanical Engineers, Part C: J. Mech. Eng. Sc.,* ***199***(33), pp. 215–223.

[8] Bukovnik, S., Dörr, N., Caika, V., Bartz, W., and Loibnegger, B., 2006. "Analysis of diverse simulation models for combustion engine journal bearings and the influence of oil condition". *Elsevier Trib. Int.,* ***39***(8), pp. 820–826.

[9] Gethin, D., 1987. "An application of the finite element method to the thermohydrodynamic analysis of a thin film cylindrical bore bearing running at high sliding speed". *ASME J. Tribol.,* ***109***, p. 283.

[10] Gandjalikhan Nassab, S., and Moayeri, M., 2002. "Three-dimensional thermohydrodynamic analysis of axially grooved journal bearings". *IMechE (Part J),* ***216***, pp. 35–47.

[11] Keogh, P., Gomiciaga, R., and Khonsari, M., 1997. "Cfd based design techniques for thermal prediction in a generic two-axial groove hydrodynamic journal bearing". *ASME J. Tribol.,* ***119***(3), pp. 428–435.

[12] Nassab, S., and Moayeri, M., 2002. "Three-dimensional thermohydrodynamic analysis of axially grooved journal bearings". *Proc. Instn Mech. Engrs, Part J: J. Eng. Tribol.,* ***216***(1), pp. 35–47.

[13] Zienkiewicz, O., 1960. "Temperature distribution within lubricating films between parallel bearing surfaces and its effect on the pressure developed". *Proc. Conference on Lubrication and Wear*.

[14] Boncompain, R., Fillon, M., and Frene, J., 1986. "Analysis of thermal effects in hydrodynamic bearings". *ASME J. Tribol.,* ***108***(2), pp. 219–224.

[15] Khonsari, M., and Wang, S., 1991. "On the fluid-solid interaction in reference to thermoelastohydrodynamic analysis of journal bearings". *ASME J. Tribol.,* ***113***, p. 398.

[16] Majumdar, B., Pai, R., and Hargreaves, D., 2004. "Analysis of water-lubricated journal bearings with multiple axial grooves". *Proc. Instn Mech. Engrs, Part J: J. Eng. Tribol.,* ***218***(2), pp. 135–146.

[17] Boncompain, R., 1984. *Les Paliers lisses en regime thermohydrodynamique aspects théoriques et experimentaux*. Poitiers.

[18] Khonsari, M., and Beaman, J., 1986. "Thermohydrodynamic analysis of laminar incompressible journal bearings". *Taylor & Francis Trib. Trans.,* ***29***(2), pp. 141–150.

[19] Gandjalikhan Nassab, S., 2005. "Inertia effect on the thermohydrodynamic characteristics of journal bearings". *Proc. of the Institution of Mechanical Engineers, Part J: J. Eng. Tribol.,* ***219***(6), pp. 459–467.

[20] Rohde, S., and Oh, K., 1975. "A thermoelastohydrodynamic analysis of a finite slider bearing". *ASME J. Lubr. Technol.,* ***97***, pp. 450–460.

[21] Fillon, M., Frêne, J., and Boncompain, R., 1987. "Historical aspects and present development on thermal effects in hydrodynamic bearings". *Fluid Film Lubrication: Proc. of the Thirteenth Lyon Symposium Tribology*, p. 27.

[22] Hirani, H., Rao, T., Athre, K., and Biswas, S., 1997. "Rapid performance evaluation of journal bearings". *Elsevier Trib. Int.,* ***30***(11), pp. 825–834.

[23] Dowson, D., 1962. "A generalized reynolds equation for fluid-film lubrication". *Elsevier Int. J. Mech. Sc.,* ***4***(2), pp. 159–170.

[24] Zengeya, M., and Gadala, M., 2007. "Optimization of journal bearings using a hybrid scheme". *Proc. Instn Mech.*

Engrs, Part J: J. Eng. Tribol., ***221***(5), pp. 591–607.
[25] Chaparro, B., Thuillier, S., Menezes, L., Manach, P., and Fernandes, J., 2008. "Material parameters identification: Gradient-based, genetic and hybrid optimization algorithms". *Comp. Mat. Sc.,* ***44***(2), pp. 339–346.
[26] Vrande, B., 2001. "Nonlinear dynamics of elementary rotor systems with compliant plain journal bearings". PhD thesis, Technische Universiteit Eindhoven.
[27] Braun, M., and Hannon, W. "Cavitation formation and modeling: a review". *Proc. Instn Mech. Engrs, Part J: J. Eng. Tribol.*, pp. 1–24.
[28] Mitchell, M., 1996. *An Introduction to Genetic Algorithms*. MIT Press, Cambridge, MA.
[29] Haupt, R., Haupt, S., and Wiley, J., 1998. *Practical Genetic Algorithms*. Wiley Online Library.
[30] TMEC. Physical properties of iso vg 46 oil. www.tmec.com/attachments/contentmanagers/331/iso46.gif.